RSC Advances

PAPER

View Article Online
View Journal | View Issue

Check for updates

Cite this: *RSC Adv.*, 2024, **14**, 16327

# Construction of a coumarin-based fluorescent probe for accurately visualizing hydrogen sulfide in live cells and zebrafish†

Xiao Wei,[ab] Long Mi,[b] Shenglong Dong,[b] Hui Yang *[b] and Shiyuan Xu*[a]

Received 26th January 2024
Accepted 13th May 2024

DOI: 10.1039/d4ra00668b

rsc.li/rsc-advances

Hydrogen sulfide ($H_2S$), an important gas signaling molecule, is a regulator of many physiological processes, and its abnormal levels are closely related to the onset and progression of disease. It is vital to develop methods for specific tracking of $H_2S$ in clinical diagnosis and treatment. In this study, we designed an ultrasensitive and highly stable coumarin-based fluorescent probe Cou-$H_2S$. Through the $H_2S$-initiated tandem reaction, Cou-$H_2S$ successfully achieved highly selective and super-fast detection of $H_2S$. Cou-$H_2S$ was successfully applied to the monitoring of endogenous and exogenous $H_2S$ at the cellular level and verified the validity of the detection of $H_2S$ in the LPS-induced zebrafish model. Therefore, Cou-$H_2S$ might provide new insights into the study of $H_2S$-related diseases.

## Introduction

Reactive sulfur species (RSS) play a pivotal role as signaling molecules in redox regulation, including hydrogen sulfide ($H_2S$), glutathione (GSH), cysteine (Cys), and sulfane sulfur.[1–3] Among them, $H_2S$ stands out as the simplest biothiol involved in the regulation of a range of complex pathophysiological processes in living organisms.[4–6] These processes include regulation of vascular tone, cytoprotection, and neurotransmission, and so on.[7–9] For example, $H_2S$ induces vascular relaxation, lowers blood pressure, and plays an important protective role in cardiovascular diseases. It effectively resists oxidative stress and protects cells and tissues.[10,11] Endogenous $H_2S$ is catalytically produced by intracellular sulfate-reducing enzymes or thioredoxin proteins (cystathionine β-synthase, cystathionine γ-lyase, and 3-mercaptopyruvate sulfur transferase).[12,13] Abnormal $H_2S$ concentrations in human serum can induce several diseases such as cardiovascular, neurological, and cancer.[14] Therefore, the development of visual detection tools to monitor intracellular $H_2S$ levels is crucial for understanding disease mechanisms and enabling early diagnosis.

Common detection methods for $H_2S$ include chromatography, electrochemistry, and mass spectrometry. Although the above methods can detect the concentration of $H_2S$ *in vitro*, they can cause damage to biological samples.[15,16] Fluorescence imaging, with its high sensitivity, high accuracy, and non-invasiveness, enables real-time, non-invasive monitoring of $H_2S$ in organisms. Based on chemical properties such as reducibility, nucleophilicity and metal coordination, researchers have developed a series of $H_2S$ fluorescent probes.[17–25] However, some of the reported probes have the disadvantages of environmental sensitivity, long reaction time, high detection limit, and the need for large amounts of organic solvents as co-solvents. It is still necessary to develop new small-molecule fluorescent probes for $H_2S$ that can overcome these limitations.

Trifluoromethyl coumarin, with the advantages of high chemical stability, wide emission wavelength range, and high

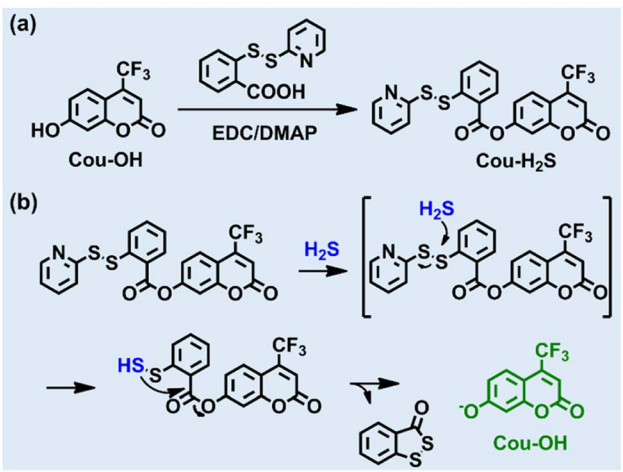


Scheme 1 (a) Synthesis of Cou-$H_2S$. (b) Reaction mechanism of Cou-$H_2S$ toward $H_2S$.

[a]*Department of Anesthesiology, Zhujiang Hospital of Southern Medical University, Guangzhou, 510282, China*

[b]*Central South University Xiangya School of Medicine Affiliated Haikou Hospital, The First Affiliated Hospital of Hainan Medical University, Haikou, 570102, China. E-mail: 15298989046@163.com; xsy998@smu.edu.cn*

† Electronic supplementary information (ESI) available. See DOI: https://doi.org/10.1039/d4ra00668b

Open Access Article. Published on 20 May 2024. Downloaded on 12/9/2025 10:08:37 AM.
This article is licensed under a Creative Commons Attribution-NonCommercial 3.0 Unported Licence.

Open Access Article. Published on 20 May 2024. Downloaded on 12/9/2025 10:08:37 AM.
This article is licensed under a Creative Commons Attribution-NonCommercial 3.0 Unported Licence.

fluorescence quantum yield, has been widely used in bioimaging and fluorescent probes.[26–31] In this work, we designed and synthesized a novel coumarin-based fluorescent probe Cou-$H_2S$ using trifluoromethyl coumarin as the molecular scaffold and 2-pyridyl disulfide as the $H_2S$ recognition group (Scheme 1). The reaction of Cou-$H_2S$ with $H_2S$ released a trifluoromethyl coumarin dye that emitted intense fluorescence at 498 nm. Cou-$H_2S$ presented excellent selectivity and sensitivity to $H_2S$, with a low detection limit of 25 nM. Cou-$H_2S$ could also be employed for fluorescence imaging of endogenous and exogenous $H_2S$ in cells. Furthermore, the upregulation of $H_2S$ levels in LPS-stimulated zebrafish was visualized.

## Experimental section

### Synthesis of 2-oxo-4-(trifluoromethyl)-2*H*-chromen-7-yl 2-(pyridin-2-yldisulfanyl)benzoate (Cou-$H_2S$)

Cou-OH (115 mg, 0.5 mmol) and 2-(pyridin-2-yldisulfanyl) benzoic acid (158 mg, 1.2 mmol) were dissolved in dry dichloromethane (20 mL). Subsequently, EDC (383 mg, 2.0 mmol) and DMAP (25 mg) were added. The reaction mixture was stirred at room temperature for 10 h. After completion of the reaction, the solvent was evaporated *in vacuo*. The resulting product was purified by silica gel column chromatography (eluent: 20% ethyl acetate/80% petroleum ether) to afford the desired compound (76 mg, 32% yield). $^1$H NMR (400 MHz, $CDCl_3$): $\delta$ 8.49–8.47 (m, 1H), 8.30 (dd, $J$ = 8.0, 1.5 Hz, 1H), 8.01 (dd, $J$ = 8.2, 1.1 Hz, 1H), 7.82(dd, $J$ = 8.8, 1.8 Hz, 1H), 7.61–7.53 (m, 3H), 7.41–7.32 (m, 3H), 7.13–7.10 (m, 1H), 6.82 (s, 1H); $^{13}$C NMR (100 MHz, $CDCl_3$): $\delta$ 163.83, 158.57, 158.44, 155.09, 153.87, 149.72, 142.14, 137.35, 134.34, 132.14, 126.40, 126.35, 125.97, 125.32, 121.14, 119.97, 119.78, 119.23, 115.55, 115.49, 111.59, 111.32; HRMS $m/z$: $C_{22}H_{12}F_3NO_4S_2$ $[M + H]^+$ calcd for 476.0238 found 476.0282.

## Results and discussion

### Design and synthesis of Cou-$H_2S$

The chemical structure of Cou-$H_2S$ was well characterized by NMR and HRMS, as shown in Fig. S1–S4.† 2-Pyridyl disulfide masked the hydroxyl group of the fluorescent dye, quenching the fluorescence of Cou-OH. The addition of $H_2S$ induced the release of Cou-OH from Cou-$H_2S$. The general mechanism was as follows: $H_2S$ reacted with Cou-$H_2S$ *via* a nucleophilic substitution reaction to give Cou-SSH intermediate, followed by an intramolecular esterification reaction to release Cou-OH and 3*H*-benzo[*c*][1,2]dithiol-3-one. To elucidate the reaction mechanism, we conducted mass spectrometry analysis of the products before and after the reaction of Cou-$H_2S$ with $H_2S$. As seen in Fig. S5,† Cou-$H_2S$ exhibited a main peak at $m/z$ = 476.0282, corresponding to Cou-$H_2S$. After the excess $H_2S$ reacted with Cou-$H_2S$, the solution showed two main peaks at $m/z$ = 167.9695 and $m/z$ = 253.0014, attributed to 3*H*-benzo[*c*][1,2]dithiol-3-one ($[M]^+$) and Cou-OH ($[M + Na]^+$).

### Optical response of Cou-$H_2S$ to $H_2S$

The response time serves as a crucial metric for assessing the probe's performance, providing insight into the kinetic process of its binding to target analytes. Upon synthesizing Cou-$H_2S$, we opted for an initial concentration of 10 μM and recorded the time course of Cou-$H_2S$ in the absence or presence of 20 μM $Na_2S$ (an inorganic $H_2S$ donor substance) in the PBS solution containing 100 μM hexadecyl trimethyl ammonium bromide (CTAB). The fluorescence intensity at 498 nm of Cou-$H_2S$ remained constant for 300 s (Fig. 1a). When 20 μM $Na_2S$ was added, the fluorescence intensity at 498 nm reached the maximum at 100 s and remained stable. The changes in fluorescence intensity before and after the reaction of Cou-$H_2S$ with $Na_2S$ across various pH values were then explored. As seen in

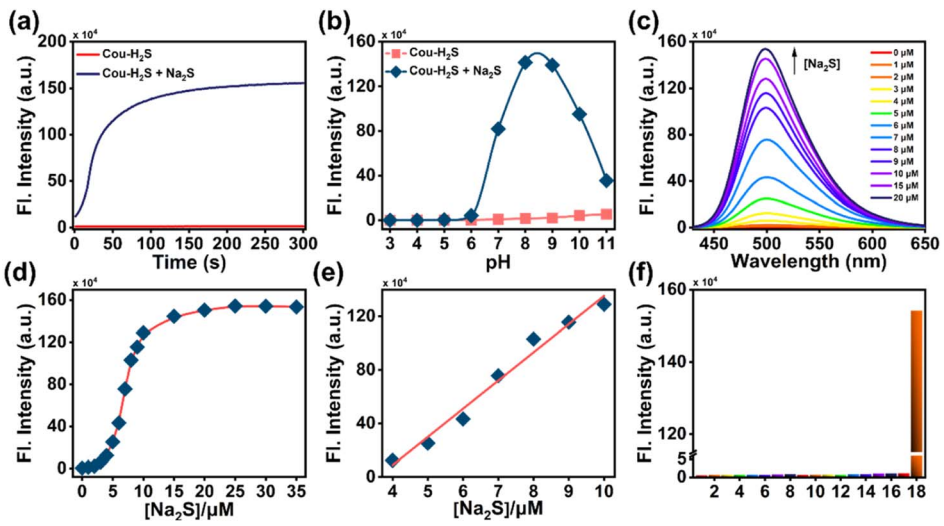


Fig. 1 (a) Fluorescence intensities at 498 nm of Cou-$H_2S$ (10 μM) in the presence or absence of $Na_2S$ (20 μM). (b) pH-dependent fluorescence intensities of Cou-$H_2S$ (10 μM) in the absence or presence of $Na_2S$ (20 μM). (c) Fluorescence response of Cou-$H_2S$ (10 μM) to varying concentrations of $Na_2S$ (0–20 μM). (d) Plot of fluorescence intensities of Cou-$H_2S$ (10 μM) at 498 *versus* $Na_2S$ concentrations (0–35 μM). (e) Linear relationship between fluorescence intensities of Cou-$H_2S$ (10 μM) at 498 nm and $Na_2S$ concentrations (4–10 μM). (f) Fluorescence response of Cou-$H_2S$ (10 μM) at 498 nm to common interfering analytes (100 μM, respectively). (1) Blank, (2) Met, (3) Gly, (4) Arg, (5) Pro, (6) $S_2O_3^{2-}$, (7) $SO_3^{2-}$, (8) $SO_4^{2-}$, (9) $Cl^-$, (10) $Mg^{2+}$, (11) $Al^{3+}$, (12) $Ca^{2+}$, (13) $Fe^{3+}$, (14) $ClO^-$, (15) Cys, (16) Hcy, (17) GSH, (18) $H_2S$. $\lambda_{ex}$ = 405 nm.


© 2024 The Author(s). Published by the Royal Society of Chemistry

Open Access Article. Published on 20 May 2024. Downloaded on 12/9/2025 10:08:37 AM.
This article is licensed under a Creative Commons Attribution-NonCommercial 3.0 Unported Licence.

Fig. 1b, the fluorescence intensity of Cou-$H_2S$ showed minimal variation over a wide pH range from 3.0 to 10.0, highlighting its insensitivity to the pH of the detection system. In the presence of $Na_2S$, the fluorescence intensity closely resembled free Cou-$H_2S$ within the pH range of 3.0–6.0. A notable increase in fluorescence intensity was observed beyond pH 6.0, reaching its peak at pH 8.0–9.0. The absorption spectra of Cou-$H_2S$ changed significantly before and after the addition of $Na_2S$ (Fig. S6†). The relationship between fluorescence intensity changes of Cou-$H_2S$ and $Na_2S$ concentration was also investigated (Fig. 1c). Under the excitation light of 405 nm, the fluorescence of the free Cou-$H_2S$ was weak. Upon sequentially adding different concentrations of $Na_2S$, the fluorescence emission peak of Cou-$H_2S$ at 498 nm gradually enhanced (Fig. 1d). In the $Na_2S$ concentration range of 0–20 μM, the fluorescence of Cou-$H_2S$ at 498 nm increased by 340-fold. This substantial change indicated a high signal-to-noise ratio for the *in vitro* detection of $H_2S$. In addition, the fluorescence intensities of Cou-$H_2S$ at 498 nm displayed an excellent linear relationship with the $Na_2S$ concentration (4–10 μM), represented by the linear equation $y/10^4 = 21.07x - 75.49$ (where $y$ was the recorded fluorescence intensity at 498 nm, and $x$ was the $Na_2S$ concentration), yielding a linear correlation coefficient of 0.99 (Fig. 1e). Utilizing the detection limit formula $3\sigma/k$ ($\sigma$ represented the standard deviation of the recorded fluorescence intensity of free Cou-$H_2S$ at 498 nm 12 times, and $k$ represented the slope of the linear equation), it could be concluded that the detection limit was 25 nM, lower than that of several reported fluorescent probes for $H_2S$ (Table S1†). To evaluate the selectivity of Cou-$H_2S$ toward $H_2S$, the performance of Cou-$H_2S$ was tested in response to common interfering analytes, including amino acids (Met, Gly, Arg, Pro), anions ($S_2O_3^{2-}$, $SO_3^{2-}$, $SO_4^{2-}$, $Cl^-$), metal ions ($Mg^{2+}$, $Al^{3+}$, $Ca^{2+}$, $Fe^{3+}$), reactive oxygen species ($ClO^-$), and biothiols (Cys, Hcy, GSH). As depicted in Fig. 1f, there was no significant variation in the fluorescence intensity at 498 nm for amino acids, anions, metal ions, and reactive oxygen species, and only $Na_2S$ triggered an enhancement of fluorescence intensity. These results underscore the excellent sensitivity and selectivity of Cou-$H_2S$ for $H_2S$, suggesting its potential use in complex biological environments.

### $H_2S$ imaging in live cells

Evaluating the cytotoxicity of Cou-$H_2S$ would provide a basis for its potential biological applications. Fig. S7† showed that incubation with different concentrations ranging from 0 to 30 μM of Cou-$H_2S$ for 24 h resulted in more than 90% cell survival, confirming the commendable biocompatibility of Cou-$H_2S$ in cellular and *in vivo* imaging experiments. As illustrated in Fig. 2, co-incubating Cou-$H_2S$ with HeLa cells yielded weak green fluorescence. When the cells were pre-incubated with Cys, followed by incubation with Cou-$H_2S$, a moderate green fluorescence emerged due to the conversion of Cys to $H_2S$ catalyzed by the thiosulfate transferase enzyme. Notably, the cells treated with $Na_2S$ induced robust green fluorescence, whereas treatment with $Na_2S$ and $ZnCl_2$ (an $H_2S$ scavenger) in turn led to reduced green fluorescence. The results established the

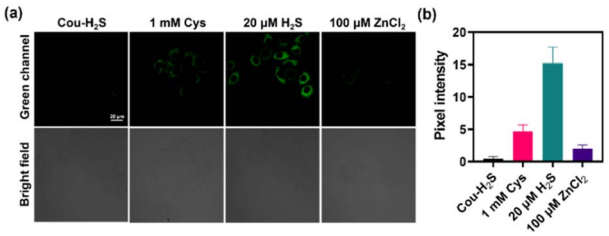


Fig. 2 Confocal laser fluorescence imaging of HeLa cells under different pretreatments. (a) The cells were treated with Cys (1 mM, 30 min), $Na_2S$ (20 μM, 30 min), $ZnCl_2$ (20 μM $Na_2S$ + 100 μM $ZnCl_2$, 30 min) at 37 °C respectively, then incubated with Cou-$H_2S$ (10 μM) and CTAB (50 μM) for 30 min before imaging. (b) Pixel intensities of the cells in plane a. $\lambda_{ex} = 405$ nm, $\lambda_{em} = 450–550$ nm. Scale bar: 20 μm.

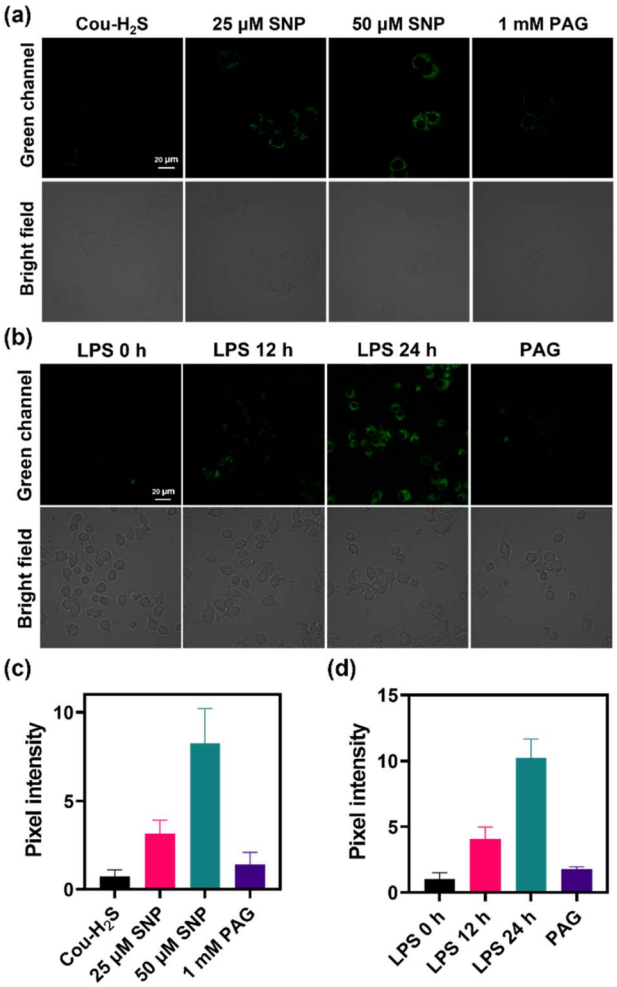


Fig. 3 (a) HeLa cells were treated with SNP (25, 50 μM, 30 min), SNP (50 μM, 30 min) + PAG (1 mM, 30 min) at 37 °C respectively, then incubated with Cou-$H_2S$ (10 μM) and CTAB (50 μM) for 30 min before imaging. (b) RAW264.7 cell were stimulated with LPS (1 μg $mL^{-1}$, 0, 12, 24 h), LPS (1 μg $mL^{-1}$, 24 h) + PAG (1 mM, 30 min) at 37 °C respectively, then incubated with Cou-$H_2S$ (10 μM) and CTAB (50 μM) for 30 min before imaging. (c) Pixel intensities of the cells in plane a. (d) Pixel intensities of the cells in plane c. $\lambda_{ex} = 405$ nm, $\lambda_{em} = 450–550$ nm. Scale bar: 20 μm.

© 2024 The Author(s). Published by the Royal Society of Chemistry

Open Access Article. Published on 20 May 2024. Downloaded on 12/9/2025 10:08:37 AM.
This article is licensed under a Creative Commons Attribution-NonCommercial 3.0 Unported Licence.

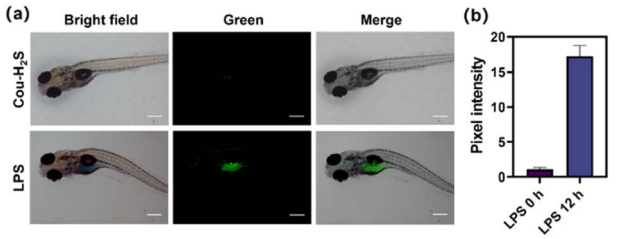


Fig. 4 (a) The zebrafish were stimulated with LPS (2 μg $mL^{-1}$) for 12 h at 37 °C, then incubated with Cou-$H_2S$ (10 μM) for 30 min before imaging. (d) Pixel intensities of the cells in plane a. $\lambda_{ex}$ = 405 nm, $\lambda_{em}$ = 450–550 nm. Scale bar: 200 μm.

capability of Cou-$H_2S$ to image exogenous $H_2S$, positioning it for biological applications.

Sodium nitroprusside (SNP) was a commonly used nitric oxide (NO) donor that induced hydrogen sulfide production.[32] Fig. 3a revealed a faint green fluorescence upon incubating the cells with Cou-$H_2S$, with varying concentrations of SNP leading to distinct enhancements in green fluorescence. Treatment of 50 μM SNP followed by propargylglycine (PAG, an $H_2S$ scavenger)[33] resulted in a rapid decline in green fluorescence, demonstrating the ability of Cou-$H_2S$ to monitor SNP-induced endogenous $H_2S$ (Fig. 3c).

Lipopolysaccharide (LPS) induced a cellular immune response leading to upregulation of $H_2S$ expression in RAW264.7 cells.[34] As displayed in Fig. 3b, faint green fluorescence was observed in RAW264.7 cells incubated with Cou-$H_2S$. When the cells were stimulated with LPS for 12 h or 24 h, and then incubated with Cou-$H_2S$, green fluorescence showed a gradual enhancement compared to that of the control group (Fig. 3d). Conversely, treatment with PAG post-LPS exposure led to a reduction in green fluorescence, highlighting Cou-$H_2S$'s ability to track the LPS-induced upregulation of $H_2S$ levels in this cellular inflammation model.

### $H_2S$ imaging in zebrafish

LPS induced up-regulation of the expression and activity of $H_2S$ synthase in zebrafish, thereby promoting $H_2S$ production. As depicted in Fig. 4, Cou-$H_2S$ was incubated with zebrafish, only weak green fluorescence was observed, likely due to the release of trifluoromethyl coumarin dye from the reaction between the low concentration of endogenous $H_2S$ and Cou-$H_2S$. The green fluorescence of zebrafish treated with LPS for 12 h increased rapidly compared to free Cou-$H_2S$. This enhancement was attributed to the significant increase in the endogenous $H_2S$ concentration in zebrafish stimulated with LPS. The findings suggested that Cou-$H_2S$ was capable of tracking changes in $H_2S$ concentration levels *in vivo*.

## Conclusions

In summary, we have designed and synthesized a novel fluorescence probe, namely Cou-$H_2S$, for the detection of $H_2S$ based on trifluoromethyl coumarin dye. Cou-$H_2S$ showed high specificity for $H_2S$, which overcame the interference of common biological analytes, such as metal ions, anions, amino acids, reactive oxygen species, and biothiols. Cou-$H_2S$ responded rapidly to $H_2S$ with response times as low as 100 s. In addition, the negligible cytotoxicity of Cou-$H_2S$ made it suitable for imaging exogenous and endogenous $H_2S$ in live cells. With the aid of Cou-$H_2S$, LPS-induced upregulation of endogenous $H_2S$ levels in zebrafish was verified. This work developed a powerful chemical tool for dynamic monitoring of $H_2S$ levels in cells and zebrafish, underpinning the study of $H_2S$-related diseases.

## Conflicts of interest

The authors declare that they have no known competing financial interests or personal relationships that could have appeared to influence the work reported in this paper.

## Acknowledgements

This research was funded by the Scientific Research Project of Health and Family Planning Industry in Hainan Province (21A200120) and Hainan Province Clinical Medical Center (2021).

## References

1 T. V. Mishanina, M. Libiad and R. Banerjee, *Nat. Chem. Biol.*, 2015, **11**, 457–464.
2 M. Iciek, A. Bilska-Wilkosz, M. Kozdrowicki and M. Górny, *Biosci. Rep.*, 2022, **42**, BSR20221006.
3 M. Iciek, A. B. Wilkosz, M. Kozdrowicki and M. Gorny, *Antioxid. Redox Signaling*, 2023, **39**, 1000–1023.
4 P. Rose, P. K. Moore and Y. Z. Zhu, *Cell. Mol. Life Sci.*, 2017, **74**, 1391–1412.
5 R. Wang, *Antioxid. Redox Signaling*, 2010, **12**, 1061–1064.
6 L. Alvarez, C. L. Bianco, J. P. Toscano, J. Lin, T. Akaike and J. M. Fukuto, *Antioxid. Redox Signaling*, 2017, **27**, 622–633.
7 L. Zhang, Y. Wang, Y. Li, L. Li, S. Xu, X. Feng and S. Liu, *Front. Pharmacol.*, 2018, **9**, 1066.
8 S. J. Tripathi, S. Chakraborty, E. Miller, A. A. Pieper and B. D. Paul, *Br. J. Pharmacol.*, 2023, 1–18.
9 J. W. Calvert, W. A. Coetzee and D. J. Lefer, *Antioxid. Redox Signaling*, 2010, **12**, 1203–1217.
10 Z. Zhao, W. Guo, C. Xu, Q. Wang, C. Mao and M. Wan, *Chem. Eng. J.*, 2023, **452**, 139089.
11 J. L. Wallace and R. Wang, *Nat. Rev. Drug Discovery*, 2015, **14**, 329–345.
12 H. Liu, M. N. Radford, C. T. Yang, W. Chen and M. Xian, *Br. J. Pharmacol.*, 2019, **176**, 616–627.
13 P. Kamoun, *Amino Acids*, 2004, **26**, 243–254.
14 X. Cao, Z. Z. Xie, Y. Yang, M. Whiteman, P. K. Moore and J. S. Bian, *Antioxid. Redox Signaling*, 2019, **31**, 1–38.
15 H. M. Smith and M. D. Pluth, *JACS Au*, 2023, **3**, 2677–2691.
16 H. Ibrahim, A. Serag and M. A. Farag, *J. Adv. Res.*, 2021, **27**, 137–153.
17 K. Shimamoto and K. Hanaoka, *Nitric Oxide*, 2015, **46**, 72–79.
18 T. T. Jia, Y. Zhang, J.-T. Hou, H. Niu and S. Wang, *Front. Chem.*, 2023, **11**, 1126309.


© 2024 The Author(s). Published by the Royal Society of Chemistry

Open Access Article. Published on 20 May 2024. Downloaded on 12/9/2025 10:08:37 AM.
This article is licensed under a Creative Commons Attribution-NonCommercial 3.0 Unported Licence.

19 D. A. Jose, R. Sakla, N. Sharma, S. Gadiyaram, R. Kaushik and A. Ghosh, *ACS Sens.*, 2020, **5**, 3365–3391.
20 J. Wang, F. Huo, Y. Yue and C. Yin, *Luminescence*, 2020, **35**, 1156–1173.
21 H. Li, Y. Fang, J. Yan, X. Ren, C. Zheng, B. Wu, S. Wang, Z. Li, H. Hua, P. Wang and D. Li, *TrAC, Trends Anal. Chem.*, 2021, **134**, 116117.
22 C. Liu, J. Pan, S. Li, Y. Zhao, L. Y. Wu, C. E. Berkman, A. R. Whorton and M. Xian, *Angew. Chem., Int. Ed.*, 2011, **50**, 10327–10329.
23 Y. Luo, Y. Zuo, G. Shi, H. Xiang and H. Gu, *Anal. Bioanal. Chem.*, 2022, **414**, 2809–2839.
24 Q. Sun, H. Liu, Y. Qiu, J. Chen, F.-S. Wu, X. G. Luo and D. W. Wang, *Spectrochim. Acta A*, 2021, **254**, 119620.
25 X. Zhang, W. Qu, H. Liu, Y. Ma, L. Wang, Q. Sun and F. Yu, *Anal. Chim. Acta*, 2020, **1109**, 37–43.
26 A. Majhi, K. Venkateswarlu and P. Sasikumar, *J. Fluoresc.*, 2023, DOI: **10.1007/s10895-023-03372-3**.
27 G. Kaur, I. Singh, R. Tandon and N. Tandon, *Inorg. Chem. Commun.*, 2023, **158**, 111480.
28 M. López-Corrales, A. Rovira, A. Gandioso, S. Nonell, M. Bosch and V. Marchán, *J. Org. Chem.*, 2023, **88**, 7128–7140.
29 A. Rovira, M. Pujals, A. Gandioso, M. López-Corrales, M. Bosch and V. Marchán, *J. Org. Chem.*, 2020, **85**, 6086–6097.
30 A. Gandioso, R. Bresolí-Obach, A. Nin-Hill, M. Bosch, M. Palau, A. Galindo, S. Contreras, A. Rovira, C. Rovira, S. Nonell and V. Marchán, *J. Org. Chem.*, 2018, **83**, 1185–1195.
31 Y. Fan, Y. Wu, J. Hou, P. Wang, X. Peng and G. Ge, *Coord. Chem. Rev.*, 2023, **480**, 215020.
32 A. D. Ivankovich, D. J. Miletich and J. H. Tinker, *Int. Anesthesiol. Clin.*, 1978, **16**, 1–29.
33 Q. Sun, R. Collins, S. Huang, L. Holmberg-Schiavone, G. S. Anand, C. H. Tan, S. van-den-Berg, L. W. Deng, P. K. Moore, T. Karlberg and J. Sivaraman, *J. Biol. Chem.*, 2009, **284**, 3076–3085.
34 Y. Zheng, N. Luo, D. Mu, P. Jiang, R. Liu, H. Sun, S. Xiong, X. Liu, L. Wang and Y. Chu, *In Vitro Cell. Dev. Biol.: Anim.*, 2013, **49**, 679–688.

© 2024 The Author(s). Published by the Royal Society of Chemistry